



**HAL**  
open science

# Numerical groundwater flow modeling for managing the Gages Jeffara aquifer system (Tunisia) in relation with oasis ecosystems

Jean-François F Vernoux, Faten Horriche, R Ghoudi

► **To cite this version:**

Jean-François F Vernoux, Faten Horriche, R Ghoudi. Numerical groundwater flow modeling for managing the Gages Jeffara aquifer system (Tunisia) in relation with oasis ecosystems. *Hydrogeology Journal*, 2020. hal-02509375

**HAL Id: hal-02509375**

**<https://brgm.hal.science/hal-02509375v1>**

Submitted on 17 Mar 2020

**HAL** is a multi-disciplinary open access archive for the deposit and dissemination of scientific research documents, whether they are published or not. The documents may come from teaching and research institutions in France or abroad, or from public or private research centers.

L'archive ouverte pluridisciplinaire **HAL**, est destinée au dépôt et à la diffusion de documents scientifiques de niveau recherche, publiés ou non, émanant des établissements d'enseignement et de recherche français ou étrangers, des laboratoires publics ou privés.



## 28 **1. Introduction**

29 Significant groundwater resources are located in southern Tunisia, but these resources, which are the main  
30 supplies in the Middle East and North Africa (MENA) coastal region, are under growing pressure in  
31 response to population and economic growth (Lezzaik and Milewski 2018). Most groundwater is taken  
32 from deep wells, which provide considerable economic advantages to the users for irrigation, domestic and  
33 industrial water supplies. Due to the climatic conditions, no sustainable agricultural production is possible  
34 without irrigation. Approximately 25% of the total area of the Gabes Jeffara plain is used for agricultural  
35 purposes with 151 irrigated areas covering 22,000 ha (Vernoux et al. 2017a). All water is drawn exclusively  
36 from shallow and deep aquifers. Since the end of the nineteenth century, many springs have been used to  
37 supply all water needs for agricultural and domestic use. Currently, all of these springs have dried up, and  
38 groundwater from deep aquifers has become the major water supply source. Groundwater resources in the  
39 Gabes region are less renewable resources. These resources are contained in Mio-Pliocene sands, Senonian  
40 limestones, Turonian dolomites, and Jurassic limestones (Vernoux et al. 2017b). The Intercalary  
41 Continental aquifer (CI), which is one of the two principal deep aquifers of the region, is considered a major  
42 contributor to the water inflow of Gabes Jeffara, and considered the Tunisian outlet of the North-Western  
43 Sahara Aquifer System (NWSAS) (Mamou et al. 2006; Ben Hamouda et al. 2013).

44 The socioeconomic development of the Gabes region has led to overexploitation of the coastal aquifers,  
45 which has induced a drying up of the springs that supplied the oases (Bayrem et al. 2015). Currently, the  
46 water extraction rate far exceeds the water recharge rate, resulting in gradual aquifer depletion, degraded  
47 water quality and seawater intrusion (Ben Alaya et al. 2014; Agoubi et al. 2013; Werner et al. 2013).  
48 Another negative impact is the degradation of oasis ecosystems, which are strongly related to groundwater  
49 (Abdedaiem 2016; Mekki et al. 2013).

50 The objective of this study was to improve the groundwater resources management in the Gabes area, taking  
51 into account the needs of socioeconomic activities and the sustainable preservation of coastal oasis  
52 ecosystems (Vernoux et al. 2017c). An important part of this study was devoted to developing a numerical  
53 flow model of the Jeffara aquifers to be used as a future groundwater management tool considering different  
54 scenarios of recharge or exploitation.

## 55 **2. Materials and Methods**

### 56 **2.1 Study area**

57 The aquifers of Gabes Jeffara are located in southeastern Tunisia and extend for approximately 3500 km<sup>2</sup>  
58 (Fig. 1). The study area is limited by El Akarit wadi and Jebel Zimla in the north, the Mediterranean Sea  
59 coast in the east, and El Hamma faults and Jebel Aziza to the west. The southern limit consists of Zeuss  
60 wadi and the Matmata mountains. Representing part of the Jeffara coastal plain of Tunisia, the region has  
61 undergone an arid to semi-arid climate change marked by seasonal contrasting climatic variables.  
62 Additionally, this area is influenced by dry/hot and humid air masses coming from the desert and from the  
63 Mediterranean Sea, respectively (Kallel 2003).

64

65

## 66 **2.2 Geological and hydrogeological setting**

67 The Gabes Jeffara multilayer aquifer system is formed mainly by sedimentary layers from the Jurassic,  
68 Cretaceous and Tertiary ages. The geological model developed as part of this study (Lasseur and Abbes,  
69 2014) includes 18 layers, of which four are considered major aquifers: Mio-Pliocene sands, Senonian  
70 limestones (Abid et al. 2012), Turonian limestones (Abid et al. 2011) and the Lower Cretaceous sands.  
71 There are three medium aquifers: marly-gypseous formations of the Senonian, upper Barremian sands and  
72 upper Jurassic limestones. All these formations constitute the aquifer system of Gabes Jeffara with the  
73 exception of the Lower Cretaceous sands (CI) attached to the NWSAS. These CI formations are  
74 nevertheless of capital importance because they contribute in an important way to the supply of the deep  
75 aquifer of Gabes Jeffara (Trabelsi et al. 2009). Both systems in communication in the El Hamma sector via  
76 a fault network (Fig. 2). Above the formations mentioned, there are also Quaternary formations associated  
77 with the wadis, and the coastal plain as well as the formations of the continental Quaternary intrarelief.  
78 These recent formations constitute the shallow aquifer system of Gabes Jeffara, as opposed to deep aquifers.  
79 These different formations were codified by the regional direction for agriculture development  
80 (Commissariat Régional au Développement Agricole CRDA) of Gabes according to lithostratigraphy and  
81 geographical location (Vernoux et al. 2017b).

82

83

## 84 **2.3 Data acquisition and processing**

85 This study, with a multidisciplinary nature, integrates several components from knowledge of groundwater  
86 resources, with a three-dimensional (3D) geological model and a groundwater flow model, Integrated Water  
87 Resources Management, analysis of water consumption, irrigated agricultural production systems and oasis  
88 ecosystems.

89 All the data processed in this study were integrated into a geographic information system (GIS), including  
90 harmonized geological maps, satellite photos and irrigated perimeters.

### 91 **2.3.1 Groundwater abstraction and springs**

92 Groundwater is extracted from shallow and deep wells. The shallow aquifers' global exploitation was  
93 deduced from the 5-year frequency publications between 1980 and 2010 and for the three main shallow  
94 aquifers (Vernoux et al. 2017b). The total exploitation ranged between 10 million cubic meters (MCM)/y  
95 in 1980 and a maximum of 25 MCM/y in 2005 (Fig. 3a). The location of the shallow wells was extracted  
96 from the inventory performed in 1995 by Abidi (2004a) (Fig. 3b). The deep wells have been inventoried  
97 annually by regional water managers since 1970. The total exploitation was approximately 50 MCM/y in  
98 1970 and was more than 100 MCM/y in 2014 (Fig. 3c). This increase is due to an increased number of deep

99 wells from approximately 70 in 1970 to more than 300 in recent years (Fig. 3d). In the past, prior to 1970,  
100 Gabes Jeffara was known for many springs. The total water flow was approximately 30 MCM/y in 1970  
101 and is now almost zero (Fig. 3e). This decrease is the result of the increased pumping from wells. The most  
102 important springs are those of El Hamma and Gabes (Fig. 3f).

103

104

### 105 **2.3.2 Groundwater monitoring**

106 The groundwater level monitoring network is relatively large with approximately 230 shallow and deep  
107 wells and piezometers monitored during the period 1970-2014. However, not all the points have continuous  
108 monitoring; the measurements are conducted for an average of between 60 and 80 points yearly.

## 109 **2.4 Development of the groundwater flow model**

### 110 **2.4.1. Modeling tool and Methodology**

111 The groundwater flow model was implemented with the MODFLOW-2000 simulator, a quasi-3D finite-  
112 difference groundwater flow model (Harbaugh et al. 2000). The package Processing Modflow 8 was used  
113 for pre- and post-processing (Simcore Software 2012). MODFLOW resolves the flow equation (Eq. 1) in  
114 steady and transient states for confined/unconfined multilayered aquifers.

$$115 \quad \frac{\partial}{\partial x} \left( e_i K_{x,i} \frac{\partial h_i}{\partial x} \right) + \frac{\partial}{\partial y} \left( e_i K_{y,i} \frac{\partial h_i}{\partial y} \right) + VL_{i,i+1} (h_{i+1} - h_i) + VL_{i,i-1} (h_{i-1} - h_i) = S_i \frac{\partial h_i}{\partial t} + q_i$$

116 (Eq. 1)

117 where:  $h_i$ ,  $h_{i+1}$ , and  $h_{i-1}$  indicate the hydraulic heads [L] of layers  $i$ ,  $i+1$  and  $i-1$ , respectively;  $K_{x,i}$  and  $K_{y,i}$  the  
118 horizontal hydraulic conductivities [L/T] in  $x$  and  $y$  directions, respectively;  $e_i$  the saturated thickness;  
119  $VL_{i,i+1}$  and  $VL_{i,i-1}$  the vertical leakance coefficients [1/T];  $S_i$  the storage coefficient [-]; and  $q_i$  the source/sink  
120 term [L/T].

121 The modeling domain is based on the hydrogeological studies performed by several authors (Barthelemy  
122 and Zammouri 2015). In fact, the complexity of the Gabes Jeffara aquifers was first simplified to set up the  
123 conceptual model and boundary conditions. All collected data were analyzed and synthesized to set up the  
124 model input. The model calibration was performed in steady and transient states by referring to groundwater  
125 level monitoring and spring flow measurements for the period 1970-2014. Once calibrated, the model could  
126 be used to simulate the groundwater flow in future decades according to several scenarios of recharge and  
127 exploitation.

### 128 *2.4.2. Conceptual model*

129 The geological model enabled update of the complex structural scheme of the Gabes multilayers known as  
130 the Gabes Jeffara aquifer system. This model allowed for the characterization of several aquifers and  
131 aquitards and of the possible hydrodynamic relationship between them (Fig. 4). Aquifer 2 is mainly present

132 in the northern part of the Jeffara, aquifer 3 is present in the south, and EL Hamma-Chenchou, Oglet  
133 Merteba, Matmatas and aquifer 5 are in the Zeuss-Koutine area. The hydrodynamic analyses performed by  
134 Vernoux et al. (2017b) confirmed a significant horizontal hydraulic communications between these  
135 aquifers. Spatially, these aquifers are connected with the Quaternary aquifer (Aquifer 1) by aquitards. These  
136 analyses allowed for consideration of them as a single layer in the model. This geological model also shows  
137 the main faults, the distribution of hot springs in the El Hamma region and the relations between the Jeffara  
138 Plain and the NWSAS through the CI (Aquifer 3).

139 The conceptual model was outlined considering the geological setting and the analyses, as presented above.  
140 Three main aquifers were identified (Fig. 5). The first aquifer corresponds to the phreatic aquifer contained  
141 in the Quaternary formations, exploited by shallow wells. The second aquifer groups the many deep layers  
142 recognized in Gabes Jeffara, which are exploited by deep wells: Gabes North and South, El Hamma,  
143 Chenchou, Oglet Merteba, Matmatas and Zeuss Koutine (ZK). The last aquifer represents the CI, which is  
144 not exploited in the study area but is used to simulate the groundwater flow between Jeffara and the CI.  
145 Vertical communication can occur between the layers through fractures in aquitards. The aquifers are  
146 recharged directly by rainfall infiltration in permeable outcrops or by runoff water and by the water inflow  
147 from the CI. The natural water outlets come from springs and wadi drainage, evapotranspiration from the  
148 water table and from the sea.

#### 149 **2.4.3. Grid design and boundary conditions**

150 The model domain overlays a regular grid of 171 rows and 212 columns with 500-m square cells (Jarraya  
151 Horriche 2017). The aquifers are conceptualized of three layers with approximately 32,000 active cells.  
152 Vertical leakance between the aquifers occurs through the aquitards and mainly along the fractures.  
153 Boundary conditions were fixed according to the conceptual model as follows:

- 154 - Recharge was applied to all of the top active cells by rainfall or runoff water infiltration.
- 155 - Pumping from shallow or deep aquifers was introduced as outflow fixed fluxes with respect to the first  
156 and second layers.
- 157 - The groundwater level was fixed to zero along the coastline for the phreatic aquifer to represent the  
158 sea boundary condition. A variable head was fixed in the northwestern limit of the CI aquifer to  
159 represent the inflow from the NWSAS.
- 160 - No flux was fixed in the other boundaries except those indicated above.
- 161 - The drainage by wadis and springs ( $Q_d$ ) was represented by drainage conditions in respect of the first  
162 and second layers. It is simulated according to Eq. 2.

$$163 \quad Q_d = C_d(h - d) \quad (\text{Eq. 2})$$

164 Where:  $h$  is the hydraulic head in the cell [L],  $d$  the drain elevation [L], and  $C_d$  the drain hydraulic  
165 conductance [ $L^2/T$ ].

166 - An evapotranspiration condition was introduced in the phreatic aquifer to simulate the outflow from  
167 the water table. Evapotranspiration (ET) is simulated according to Eq. 3.

$$168 \quad ET = ET_{max} \left[ \frac{h-(Z-p)}{p} \right] \quad (\text{Eq. 3})$$

169 Where:  $ET_{max}$  indicates the maximum evapotranspiration [L/T],  $h$  the hydraulic head [L],  $Z$  the ground  
170 level [L], and  $p$  [L] the water table depth beyond which ET is null.

#### 171 **2.4.4. Groundwater recharge**

172 Gabes Jeffara is mainly recharged by rainfall infiltration in permeable outcrops or by runoff water. The  
173 latter was assessed by referring to the hydrologic study performed at the level of Gabes Jeffara watersheds  
174 (Vernoux et al. 2017b). The rainfall infiltration in permeable outcrops was deduced from an overall  
175 estimation of infiltration capacity according to the geological formations and from the field knowledge of  
176 hydrogeologists. The overall recharge was computed to an average of 16.4 MCM/y. In the groundwater  
177 flow model, this recharge was distributed within the watersheds using the water accumulation ratio deduced  
178 from the Digital Elevation Model (DEM) (Jarraya Horriche 2017). The runoff recharge in a cell was  
179 calculated according to Eq. 4. Thus, runoff water was mainly recharged in the watercourse network of each  
180 watershed. In addition to the runoff water infiltration, some areas were recognized as highly permeable  
181 outcrops favorable for direct rainfall infiltration such as the areas of Matmatas, El Hamma-Chenchou and  
182 Oudhref.

$$183 \quad R(i) = \frac{A(i)}{\sum_1^N A(i)} RW \quad (\text{Eq. 4})$$

184 Where:  $RW$  is the total runoff recharge in the watershed [L/T] and  $A(i)$  the surface accumulation water in  
185 a cell within the watershed [-] which is calculated by GIS using the DEM.

#### 186 **2.4.5. NWSAS groundwater inflow**

187 Groundwater inflow from the NWSAS occurs through the CI aquifer in the north-western limit which  
188 represents a principal inflow water source of the Jeffara aquifers. This inflow, known as the “Tunisian  
189 outlet”, goes by vertical leakance to the Jeffara aquifers through several faults mainly in the El Hamma-  
190 Chenchou areas. According to previous studies, this inflow was assessed to 3.1 m<sup>3</sup>/s (OSS, 2003) and 3.6  
191 m<sup>3</sup>/s (Besbes et al., 2005) in 1950. This last study assessed the inflow to 1.4 m<sup>3</sup>/s in 2000. In the present  
192 groundwater flow modeling, variable heads were fixed in the northwestern limit of the CI aquifer by  
193 referring to head measurements in the CI near this limit. Head values ranged between 140 and 155 m in  
194 1970 and decreased to about 60-72 m in 2014. The same tendency of measured heads was used in the fixed  
195 heads limit.

#### 196 **2.4.6. Hydrodynamic parameters**

197 The Gabes Jeffara aquifer has been investigated by many researchers since 1970, which allowed an overall  
198 assessment of the hydraulic transmissivity and storage coefficient in many regions and for some aquifers

199 (Rouatbi 1967; UNESCO 1972; Mekrazi 1974; Abidi 2004a and 2004b). Pumping tests in many deep wells  
 200 also allowed the measurement of these parameters. Abidi (2004b) summarized these studies and adopted  
 201 the average values that were used for the first calibration of the model (Table 1).

202 When referring to the groundwater flow modeling conducted for the whole Jeffara aquifer in Tunisia and  
 203 Libya (Besbes et al. 2005), the calibrated transmissivity is approximately  $4 \times 10^{-3} \text{ m}^2/\text{s}$  for the phreatic  
 204 aquifer and ranges between 1 and  $2 \times 10^{-2} \text{ m}^2/\text{s}$  for the deep aquifer. The storage coefficient was calibrated  
 205 to 0.15 for the phreatic aquifer and 0.03 for the deep aquifer.

206 **Table 1.** Average measured transmissivity and storage coefficient

Aquifer	Transmissivity ( $\text{m}^2/\text{s}$ )	Storage Coefficient
Northern Gabes (Sand layer)	$10 \times 10^{-3}$	$10^{-6} - 5 \times 10^{-4}$
Northern Gabes (Limestone layer)	$30 \times 10^{-3}$	
El Hamma-Chenchou	$40 \times 10^{-3}$	$3 \times 10^{-5} - 2 \times 10^{-4}$
Southern Gabes	$40 \times 10^{-3}$	$3 \times 10^{-5} - 10^{-2}$
Oglet Merteba	$5 \times 10^{-3}$	-
Phreatic aquifer	$9 \times 10^{-2}$	$2 \times 10^{-2} - 9 \times 10^{-2}$

207

## 208 **2.5 Calibration and validation of the groundwater flow model**

209 The model was first calibrated in steady state for 1970. During this period, the pumping rates, spring flows  
 210 and groundwater levels remained relatively stable, confirming the quasi-equilibrium of the groundwater  
 211 flow regime. In addition, most of the collected data started during this period, which is helpful for model  
 212 calibration. The model was then calibrated in transient state for the period 1971-1990, i.e., 10 periods of  
 213 one year each. 'Initial condition' corresponds to the hydraulic head calibrated during steady state. The  
 214 pumping flow rates in wells were distributed into the active cells of the shallow and deep aquifers. The  
 215 groundwater recharge was computed in transient state according to the steady state recharge and the  
 216 variation of the average annual rainfall.

217 Calibration was performed from groundwater levels measured in more than 200 wells and piezometers and  
 218 from the spring flows (Jarraya Horriche 2017). Simulated piezometric maps and water balances were also  
 219 used to calibrate performance by referring to previous studies (OSS 2003). The calibration parameters are  
 220 related to the horizontal transmissivities, the storage coefficients, the vertical leakance coefficients between  
 221 layers, the drain and ET parameters. Groundwater flow is highlighted in faults by increasing vertical  
 222 leakance parameters and decreasing horizontal transmissivities. The calibration process is manual using the  
 223 trial-and-error method. Hydrodynamic parameters are calibrated during steady state except the storage  
 224 coefficient in transient state. The recharge in transient state is calculated by using the calibrated recharge  
 225 in steady state and the annual rainfall.

226 Finally, the model was validated for the period 1991-2014 by extending the transient state until 2014.  
 227 Validation was performed using other groundwater level measurements and spring flow for this period.

## 228 **2.6 Simulation of water demand and groundwater management scenarios**



229 The analysis of current and future water consumption was carried out with existing data, the processing of  
230 satellite images, and farmer surveys (Vernoux et al. 2017a). Processed satellite images were used to assess  
231 the total areas of the different irrigated areas, the areas actually irrigated and the volumes of water  
232 consumed, when these data were not enabled.

233 Current water requirements were estimated at 125 Mm<sup>3</sup> in 2014 (baseline year), of which 82% was for the  
234 irrigated perimeters for a total irrigated area of more than 14,000 ha. Non-agricultural water requirements  
235 were estimated at 22 Mm<sup>3</sup> in 2014, of which 13 Mm<sup>3</sup> was devoted to domestic use. Water requirements for  
236 the industrial and tourism sectors were low and represented only 7% of total requirements.

237 The second step of the process consisted of identifying the main factors of changes that could influence  
238 water needs in the future and then describing their evolution trends by 2040. Three scenarios were  
239 predefined for the future (Fig. 6). The first scenario A (trend) is based on the continuation of past trends  
240 (continued urbanization of oases, increase in the area of private irrigated areas, etc.). The second scenario  
241 B (pessimistic) assumes an aggravation of past trends relative to scenario A. The third scenario C  
242 (optimistic) assumes that current and future pressures on water resources will be lower, compared to  
243 scenario A.

244 Future irrigation water needs by 2040 are estimated at a best-case scenario of 215 MCM/y (scenario C) and  
245 at a worst-case scenario of 517 MCM/y (scenario B). Considering the assumptions in the trend scenario,  
246 these needs would be 286 MCM/y in 2040.

247 Studying the functional levels of oasis ecosystems enabled definition of the links between the ecosystems  
248 and the groundwater of the Tunisian Jeffara aquifers and facilitated the proposal of a protocol for  
249 monitoring these links, through a number of indicators and predefined parameters (Abdedaiem 2016).

250 Finally, an Integrated Water Resources Management (IWRM) assessment was carried out, with the main  
251 objective of defining water demand scenarios combined with scenarios of decreased groundwater  
252 withdrawal, reinforced groundwater recharge and use of alternative water resources (Hamza 2017). These  
253 scenarios were tested with the hydrodynamic model to see their impact on groundwater levels and spring  
254 flow rates.

255 During modeling simulations, rainfall and runoff recharge were maintained constant and equal to the  
256 average value of the transient period (1970-2014). The fixed head boundary for the phreatic aquifer was  
257 the same as for the steady and transient states. For the NWSAS-CI boundary, variable fixed heads were  
258 considered by extrapolating the tendency of measured heads during the transient state for the simulation  
259 period, as a first step. In a second step, variable fixed fluxes were applied by extrapolating the tendency of  
260 calculated values by the model. All the parameters such as transmissivity, vertical leakance, storage  
261 coefficient, drainage and evapotranspiration-related parameters, were maintained the same as for the  
262 transient state. Initial condition corresponded to the hydraulic head calculated in 2014.

263

### 265 3. Results and Discussion

#### 266 3.1. Model performance assessment

267 The assessment of the model calibration was first based on the comparison of simulated and  
 268 measured groundwater levels. The mean square error (MSE) for the steady state calibration was  
 269 equal to 18 m<sup>2</sup> for the shallow aquifer and 21 m<sup>2</sup> for the deep aquifer (Figs. 7b and 7d). The  
 270 piezometric maps simulated by the model confirm the hydrodynamic functioning of the  
 271 groundwater and the drainage of the groundwater downstream of the wadis, at the level of the  
 272 wetlands and the springs (Figs. 7a and 7 c). The variation of the simulated heads and spring flows  
 273 are shown to be close to the measured values for most piezometers and springs (Figs. 8 and 9).

274 The water balance computed in steady and transient states shows that the total inflow was  
 275 approximately 4.9 m<sup>3</sup>/s in 1970, shared between rainfall recharge and inflow from the Intercalary  
 276 Continental (CI) (Tab. 2). During this period, the well pumping rate was 1.9 m<sup>3</sup>/s and computed  
 277 drainage flow mainly from springs was 1 m<sup>3</sup>/s. The remaining outflow was the evapotranspiration  
 278 from the water table in the wetland areas. In 2014, the CI inflow decreased to 0.7 m<sup>3</sup>/s because of  
 279 the decrease in the CI hydraulic heads in the northwestern boundary limits. Consequently, a  
 280 depletion of the springs and an increase of the well pumping rate to 3.9 m<sup>3</sup>/s were noticed. This  
 281 situation induced a decrease in hydraulic heads and evapotranspiration flux from the water table.  
 282 At the same time, a decrease in wetland areas was observed, compared to the 1970 scenario. The  
 283 overall water balance showed a contribution of 3.2 m<sup>3</sup>/s from the groundwater storage.

284 The model results confirm those of previous studies, especially the groundwater inflow from the  
 285 CI aquifer. The inflow was computed as 3.1 m<sup>3</sup>/s and 3.5 m<sup>3</sup>/s in 1950 according to OSS (2003)  
 286 and Besbes et al. (2005), respectively. By 2000, this inflow had decreased to 1.5 m<sup>3</sup>/s and 1.4 m<sup>3</sup>/s  
 287 in the same studies.

288

289 **Table 2** Water balances simulated by the model

Parameter	1970		2014	
	Inflow (m <sup>3</sup> /s)	Outflow (m <sup>3</sup> /s)	Inflow (m <sup>3</sup> /s)	Outflow (m <sup>3</sup> /s)
Inflow from CI	2.93	-	0.74	-
Exchange with the sea	-	0.19	0.00	0.13
Pumping total:	-	1.88	-	3.93
Pumping from shallow wells	-	0.20	-	0.69
Pumping from deep wells	-	1.68	-	3.24
Drainage total:	-	1.00	-	0.04

Drainage from wadis	-	0.04	-	0.02
Drainage from springs	-	0.96	-	0.02
Recharge	1.96	-	1.14	-
Evapotranspiration from the water table	-	1.82	-	0.99
Groundwater storage	-	-	3.20	-
<b>TOTAL</b>	<b>4.89</b>	<b>4.89</b>	<b>5.09</b>	<b>5.09</b>

290

### 291 **3.2 Simulation of groundwater management scenarios**

292 The calibrated model was used to simulate the impact of groundwater exploitation in the future according  
 293 to several management scenarios by referring to the water demand of the Gabes region (Bouzit et al., 2017).  
 294 Six scenarios were tested with the model over the period 2015-2040 (Jarraya Horriche 2017; Chaif et al.  
 295 2017). For all simulations, fixed head was kept the same along the coast for the phreatic aquifer. For rainfall  
 296 and runoff recharge, constant values were considered on the base of an average rainfall for 1970-2040.  
 297 Parameters for evapotranspiration and drainage boundary conditions were the same as those of the transient  
 298 state.

299 For scenario 1, the pumping rates were kept constant throughout the period. The inflow from the CI (the  
 300 Tunisian outlet) will be equal to 0.15 m<sup>3</sup>/s in 2040. The overall water balance deficit will be on the order  
 301 of 2 m<sup>3</sup>/s. The groundwater level will be affected by a drawdown ranging between 5 m and 15 m, mainly  
 302 near the spring areas of El Hamma. Also noted is a shrinkage of the salty wetlands (sebkhas) following the  
 303 decrease in evapotranspiration from the water table. For scenario 2, a linear increase in the pumping rates  
 304 of all the deep wells was considered, while keeping their number constant. Thus, the total pumping rate will  
 305 be equal to 5.2 m<sup>3</sup>/s in 2040. The results of this simulation show that water salinization could take place  
 306 after the higher groundwater level declines, and consequently, the inversion of the hydraulic gradient  
 307 occurs, mainly in northern Gabes. The overall areas will be affected by additional decreases in groundwater  
 308 levels, drainage and spring flows and evapotranspiration from the water table, compared to scenario 1. The  
 309 water balance deficit will be equal to 3 m<sup>3</sup>/s in 2040, and the drainage flow through wadis and springs will  
 310 be almost zero. The inflow from the CI will decrease to 0.37 m<sup>3</sup>/s in 2040 following the piezometric drops  
 311 in El Hamma.

312 Scenarios 3 and 4 are based on water demand scenarios, as defined in the socioeconomic analysis (scenarios  
 313 A and C in Fig. 6) without water resource management measures, while scenarios 5 and 6 are based on the  
 314 same water demand scenarios but with water resource management measures (Hamza, 2017). The  
 315 management measures tested in scenarios 5 and 6 can be grouped into three classes: reducing withdrawals,  
 316 enhancing recharge, and using alternative water resources, in particular seawater desalination. These  
 317 measures have been spatialized according to their nature, the targeted water tables and the concerned  
 318 administrative delegations.

319 For scenario 3, the total pumping rates will be equal to 8.9 m<sup>3</sup>/s in 2040, inducing a more critical situation  
 320 for the water balance (Tab. 3) and for groundwater level drawdown (Fig. 10a). Therefore, we considered

321 scenario 6 with water resources management measures, which (i) limit the evolution of irrigated areas, (ii)  
 322 reduce abstractions by better valorization of pumped water, both by promoting water-saving crops and by  
 323 improving the efficiency of distribution networks, (iii) reinforce recharge and (iv) use unconventional water  
 324 resources (desalination, for example). These measures can reduce groundwater abstraction by 2 to 3 m<sup>3</sup>/s  
 325 and reach in 2040 the same total pumping rate as in 2014 (Tab. 2). The results of this simulation show that  
 326 the water balance in 2040 will be similar to that of 2014 and that the groundwater level drawdown will be  
 327 reduced (Fig. 10b).

328 **Table 3** Water balances simulated by the model in 2040 for scenarios 3 and 6

Parameter	2040 – Scenario 3 (water demand scenario A without water resource management measures)		2040 – Scenario 6 (water demand scenario C with water resource management measures)	
	Inflow (m <sup>3</sup> /s)	Outflow (m <sup>3</sup> /s)	Inflow (m <sup>3</sup> /s)	Outflow (m <sup>3</sup> /s)
Inflow from CI	0.32	-	0.32	-
Exchange with the sea	0.08	0.04	0.003	0.169
Pumping total:	-	8.91	-	4.00
Pumping from shallow wells	-	0.876	-	0.08
Pumping from deep wells	-	8.037	-	3.92
Drainage total:	-	0.002	-	0.02
Drainage from wadis	-	0.002	-	0.020
Drainage from springs	-	0.000	-	0.006
Recharge	2.47	-	2.47	-
Evapotranspiration from the water table	-	0.36	-	0.95
Groundwater storage	6.45	-	2.83	-
<b>TOTAL</b>	<b>9.32</b>	<b>9.32</b>	<b>5.63</b>	<b>5.63</b>

329

330

#### 331 4. Conclusions

332 The Gabes Jeffara aquifer system, in southern Tunisia, is very important for the regional water supply.  
 333 Increasing water demand, mainly for irrigation, has led to a need for better management of this crucial  
 334 resource to prevent groundwater depletion and deteriorating effects, such as saltwater intrusion from over  
 335 pumping, in this coastal region. A groundwater flow model was developed to simulate different scenarios  
 336 of water demand and to be used as a tool for groundwater resource control and for help in planning further  
 337 exploitation of the system, including the use of nonconventional water resources.

338 The groundwater flow model is based on a 3D geological model (Lasseur and Abbes 2014) and  
 339 approximately 50 years of monitoring data: withdrawals, piezometric levels, and spring water flows. The  
 340 model was calibrated in steady state with reference to the piezometric measurements measured in 1970.  
 341 The piezometric maps plotted by the model confirm the hydrodynamic functioning of the groundwater and  
 342 the drainage of the groundwater downstream of the wadis, at the level of the wetlands and springs. The  
 343 model was calibrated in transient state for the period 1972-2014, using records from more than 200 wells

344 and piezometers. The model confirms the importance of the groundwater inflow from the Continental  
345 Intercalary (Besbes et al. 2005) and its decline (from 3 m<sup>3</sup>/s in 1970 to 0.75 m<sup>3</sup>/s in 2014).

346 The tested scenarios show that the decline in groundwater levels of the Jeffara aquifers is likely to continue,  
347 with the induced effects of reduced exploitable resources, deteriorated groundwater quality and increased  
348 operating costs. Even with an unrealistic assumption of maintaining water withdrawals at their 2014 level  
349 (Scenario 1), water table decline will continue, under the double effect of withdrawals exceeding aquifer  
350 recharge and the inexorable decline of the Continental Intercalary water supply. Nevertheless, the  
351 simultaneous implementation of management measures, with the aim of improving the use of existing  
352 resources, reinforcing recharge and bringing new resources, can, however, enable a very significant  
353 reduction in the decline of groundwater levels.

354 **Acknowledgements** The authors gratefully acknowledge FFEM (French Facility for Global Environment) and AFD  
355 (French Agency for Development) for financial support and CRDA (Regional Commissariat for Agricultural  
356 Development) of Gabes for technical support.

## 357 **References**

358 Abdedaïem S. (2016) Gestion des Aquifères côtiers des Oasis de Gabès – Analyse des écosystèmes oasiens de Gabès  
359 et de leurs relations avec les aquifères [Management of coastal aquifers in Gabes Oases - Analysis of oasis ecosystems  
360 in Gabes and their relationship with aquifers]. Report BRGM/RC-67032-FR, 85 p.

361 Abid K., Zouari K., Dulinski M., Chkir N., Abidi B. (2011) Hydrologic and geologic factors controlling groundwater  
362 geochemistry in the Turonian aquifer (southern Tunisia). *Hydrogeology Journal* 19, 415-427.  
363 <https://doi.org/10.1007/s10040-010-0668-z>

364 Abid K., Hadj Ammar F., Chkir N., Zouari K. (2012) Relationship between Senonian and deep aquifers in Southern  
365 Tunisia, *Quaternary International*, Volume 257, 2012, Pages 13-26, ISSN 1040-6182,

366 Abidi B. (2004a) Etude des nappes phréatiques de la Jeffara de Gabès [Study of the shallow groundwater of the Gabes  
367 Jeffara]. Internal report. CRDA de Gabès.

368 Abidi B. (2004b) Caractéristiques hydrodynamiques et géochimiques de la Jeffara de Gabès [Hydrodynamic and  
369 geochemical characteristics of the Gabes Jeffara]. Internal report. CRDA de Gabès.

370 Agoubi B., Kharroubi A., Abichou t., Abida H. (2013) Hydrochemical and geoelectrical investigation of Marine  
371 Jeffara Aquifer, southeastern Tunisia. *Applied Water Science*, 3(2): 415-429, <https://doi.org/10.1007/s13201-013-0091-4>

373 Barthélemy Y., Zammouri M. (2015) – Projet de Gestion des Aquifères côtiers des Oasis de Gabès –Synthèse des  
374 modèles existants et préfiguration du modèle hydrogéologique conceptuel [Management of coastal aquifers in Gabes  
375 Oases - Synthesis of existing models and prefiguration of the conceptual hydrogeological model]. report BRGM/RC-  
376 64551-FR, 182 p

377 Bayrem N., Moussa M., Rejeb H. (2015) The water Resources Challenges in Gabes Oasis. *Int. Res.J. Earth Sci*, 3(3) :  
378 15-19

379 Ben Alaya M., Saidi S, Zemni T, Zargouni F (2013) Suitability assessment of deep groundwater for drinking and  
380 irrigation use in the Jeffara aquifers (Northern Gabes, south-eastern Tunisia). Environ Earth Sci.  
381 <https://doi.org/10.1007/s12665-013-2729-9>

382 Ben Hamouda M., Mamou A., Bejaoui J., Froehlich K. (2013) Hydrochemical and Isotopic Study of Groundwater  
383 in the North Djeffara Aquifer, Gulf of Gabès, Southern Tunisia, International Journal of Geosciences, 4(8A):1-10.  
384 <https://doi.org/10.4236/ijg.2013.48A001>

385 Besbes, M., Bouhlila R., Pallas, P., Pizzi, G., Ayoub, A., Babasy, M., El Barouni, S. et Horriche, F. (2005) Etude sur  
386 modèles mathématiques de la Jeffara tuniso-libyenne [Study on mathematical models of Tunisian-Libyan Jeffara].  
387 OSS report.

388 Bouzit M., J.F. Vernoux, M. Sghair et M. Abdeadhim (2017) Projet de gestion des aquifères côtiers des oasis de  
389 Gabès - Analyse socio-économique et évolution future des besoins en eau du gouvernorat de Gabès [Management of  
390 coastal aquifers in Gabes Oases - Socio-economic analysis and future evolution of the water needs of Gabes  
391 governorate]. report. BRGM/RC-66708-FR, 68 p

392 Chaif H., Vernoux J.F., Jarraya Horriche F., Barthélemy Y. (2017) Gestion des Aquifères côtiers des Oasis de Gabès  
393 - Modélisation hydrodynamique : Scénarios prévisionnels basés sur des projections d'évolution de la demande en eau,  
394 avec et sans mesures de gestion [Management of coastal aquifers in Gabes Oasis – Hydrodynamic model :  
395 Previsionnel scenarios based on projected evolution of water demand, with and without management actions]. Report  
396 BRGM/RC-67186-FR, 87 p.

397 Hamza M. (2017) Projet de gestion des aquifères côtiers des oasis de Gabès – Gestion intégrée des ressources en eau  
398 et des écosystèmes associés [Management of coastal aquifers in Gabes Oases - Integrated management of water  
399 resources and associated ecosystems]. Report BRGM/RC-66280-FR, 243 pages

400 Harbaugh AW, Banta ER, Hill MC, McDonald MG (2000) MODFLOW-2000, The U.S. Geological Survey modular  
401 ground-water model: user guide to modularization concepts and the ground-water flow process. US Geological  
402 Survey, Reston, 121p

403 Jarraya Horriche F. (2017) Gestion des Aquifères côtiers des Oasis de Gabès – Modèle hydrodynamique de la Djeffara  
404 de Gabès [Management of coastal aquifers in Gabes Oasis – Hydrodynamic model of Gabes Djeffara]. Report  
405 BRGM/RC-67031-FR, 139 p.

406 Kallel R (2003) Hydrologie de la Jeffara tunisienne [Hydrology of the Tunisian Jeffara. Internal report. CRDA of  
407 Gabes

408 Lasseur E., Abbes C. (2014) Projet de gestion des aquifères côtiers des oasis de Gabès – Modélisation géologique 3D  
409 de la Jeffara de Gabès [Management of coastal aquifers in Gabes Oases - 3D geological modeling of the Gabes Jeffara.  
410 Report BRGM/RC-64626-FR, 94 p.

411 Lezzaik K, Milewski A (2018) A quantitative assessment of groundwater resources in the Middle East and North  
412 Africa region. Hydrogeol J 26:251–266. <https://doi.org/10.1007/s10040-017-1646-5>

413 Mamou A., Besbes M., Abdous B., Latrech D.J. and Fezzani C. (2006) North Western Sahara Aquifer System  
414 (NWSAS), in Non-Renewable Groundwater Resources, a guidebook on socially-sustainable management for water-

415 policy maker, edited by S. Foster and D.P. Loucks, UNESCO, 68-74 <https://fr.ircwash.org/sites/default/files/Foster->  
416 [2006-Nonrenewable.pdf#page=62](https://fr.ircwash.org/sites/default/files/Foster-2006-Nonrenewable.pdf#page=62)

417 Mekki I, Jacob F, Marlet S, Ghazouani W (2013) Management of groundwater resources in relation to oasis  
418 sustainability: the case of the Nefzawa region in Tunisia. *J Environ Manage* 121:142–151.  
419 <https://doi.org/10.1016/j.jenvman.2013.02.041>

420 Mekrazi A (1975) Contribution à l'étude géologique et hydrogéologique de la région de Gabès Nord. Thèse de  
421 Doctorat ès Sciences Géologiques, [Contribution to the hydrogeological Study of the Gabes Region North], 3rd Cycle  
422 Thesis, University of Bordeaux I., 230 p.

423 Observatoire du Sahara et du Sahel (OSS) (2003) Système Aquifère du Sahara Septentrional: Modèle mathématique,  
424 vol. IV [Aquifer System of the Northern Sahara : Mathematical model, vol. IV]. [http://www.oss-](http://www.oss-online.org/fr/syst%C3%A8me-aquif%C3%A8re-du-sahara-septentrional-mod%C3%A8le-math%C3%A9matique-volume-iv)  
425 [online.org/fr/syst%C3%A8me-aquif%C3%A8re-du-sahara-septentrional-mod%C3%A8le-math%C3%A9matique-](http://www.oss-online.org/fr/syst%C3%A8me-aquif%C3%A8re-du-sahara-septentrional-mod%C3%A8le-math%C3%A9matique-volume-iv)  
426 [volume-iv](http://www.oss-online.org/fr/syst%C3%A8me-aquif%C3%A8re-du-sahara-septentrional-mod%C3%A8le-math%C3%A9matique-volume-iv)

427 Rouatbi R. (1967) Contribution à l'étude hydrogéologique du Karst enterré de Gabès Sud. (Contribution to the Study  
428 of Hydrogeological Buried Karst of South Gabes), PhD Thesis, University of Montpellier, 235 p.

429 Simcore Software (2012) Processing Modflow. An Integrated Modeling Environment for the Simulation of  
430 Groundwater Flow, Transport and Reactive Processes. User's guide. <http://www.simcore.com/>

431 Trabelsi, R., Kacem, A., Zouari, K., Rozanski, K. (2009) Quantifying regional groundwater flow between Continental  
432 Intercalaire and Djefara aquifers in southern Tunisia using isotope methods. *Environmental Geology* 58(1): 171-183.  
433 <https://doi.org/10.1007/s00254-008-1503-x>

434 UNESCO (1972) Etude des ressources en eau du Sahara septentrional. Projet ERESS [Study of the water resources of  
435 the northern Sahara. ERESS project]. <https://unesdoc.unesco.org/ark:/48223/pf0000001564>

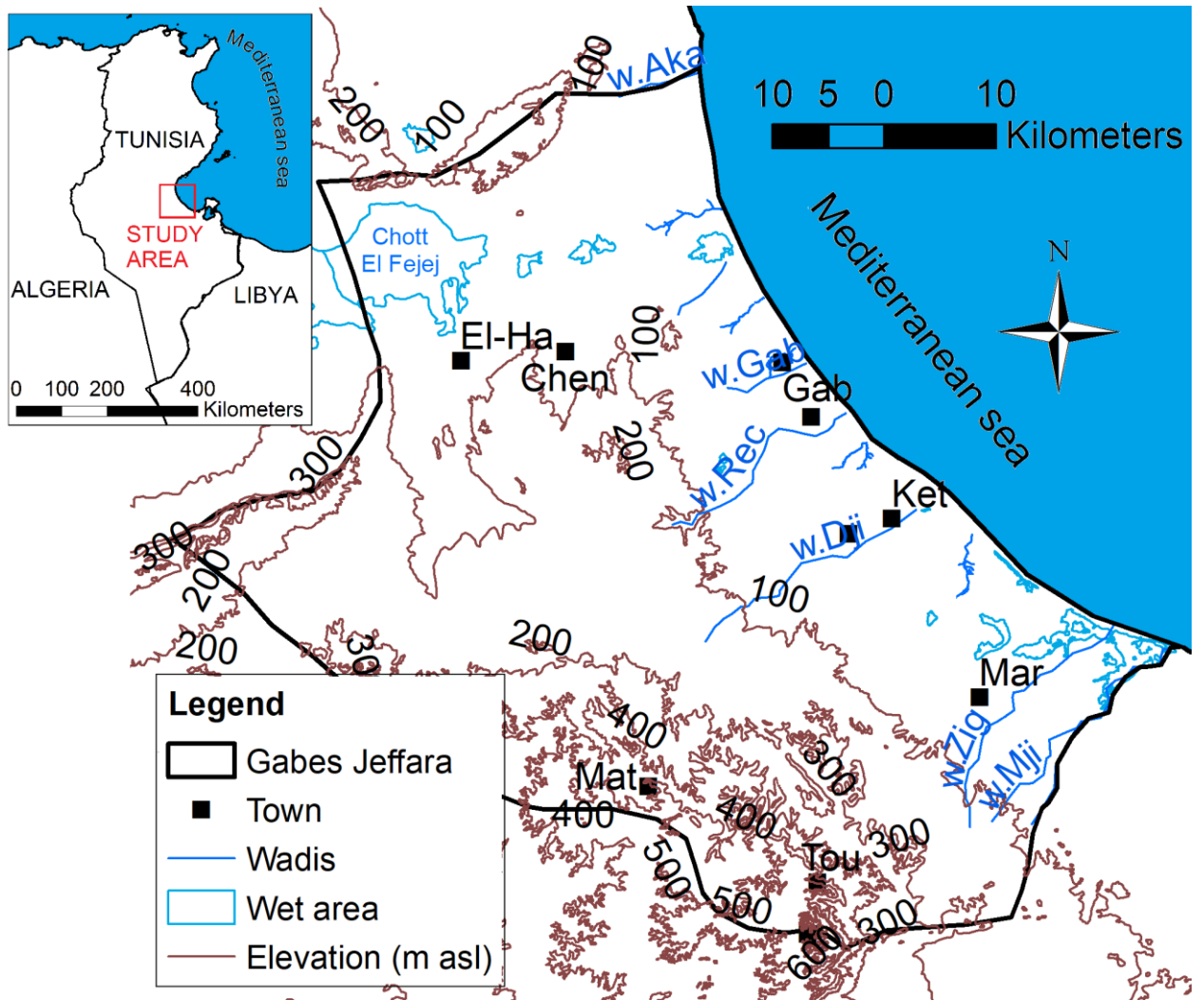
436 Vernoux J.F., Bouzit M., Desprats J.F., Ben Salah M., Sghair M., Abdeadhim M. (2017a) Gestion des Aquifères  
437 côtiers des Oasis de Gabès – Analyse des systèmes de production agricole irriguée [Management of coastal aquifers  
438 in Gabes Oases - Analysis of irrigated agricultural production systems]. Report BRGM/RC-65740-FR, 77 p.

439 Vernoux J.F., Machard de Gramont H., Barthélemy Y., Croiset N., Gourcy L., Stollsteiner P. (2017b) Gestion des  
440 Aquifères côtiers des Oasis de Gabès - Synthèse hydrogéologique [Management of coastal aquifers in Gabes Oases –  
441 Hydrogeological synthesis]. Report BRGM/RC-64953-FR, 200 p.

442 Vernoux J.F., Horriche F., Ghoudi R., Abdedaiem S., Hamza M. (2017c) Management of Gabes Jeffara aquifers in  
443 relation with oasien ecosystems. In *Recent Advances in Environmental Science from the Euro-Mediterranean and*  
444 *Surrounding Regions: Proceedings of Euro-Mediterranean Conference for Environmental Integration (EMCEI-1),*  
445 *Tunisia 2017*, p. 599-602.

446 Werner AD, Simmons CT (2009) Impact of sea-level rise on sea water intrusion in coastal aquifers. *Ground Water*  
447 47:197–204. <https://doi.org/10.1111/j.1745-6584.2008.00535x>

448

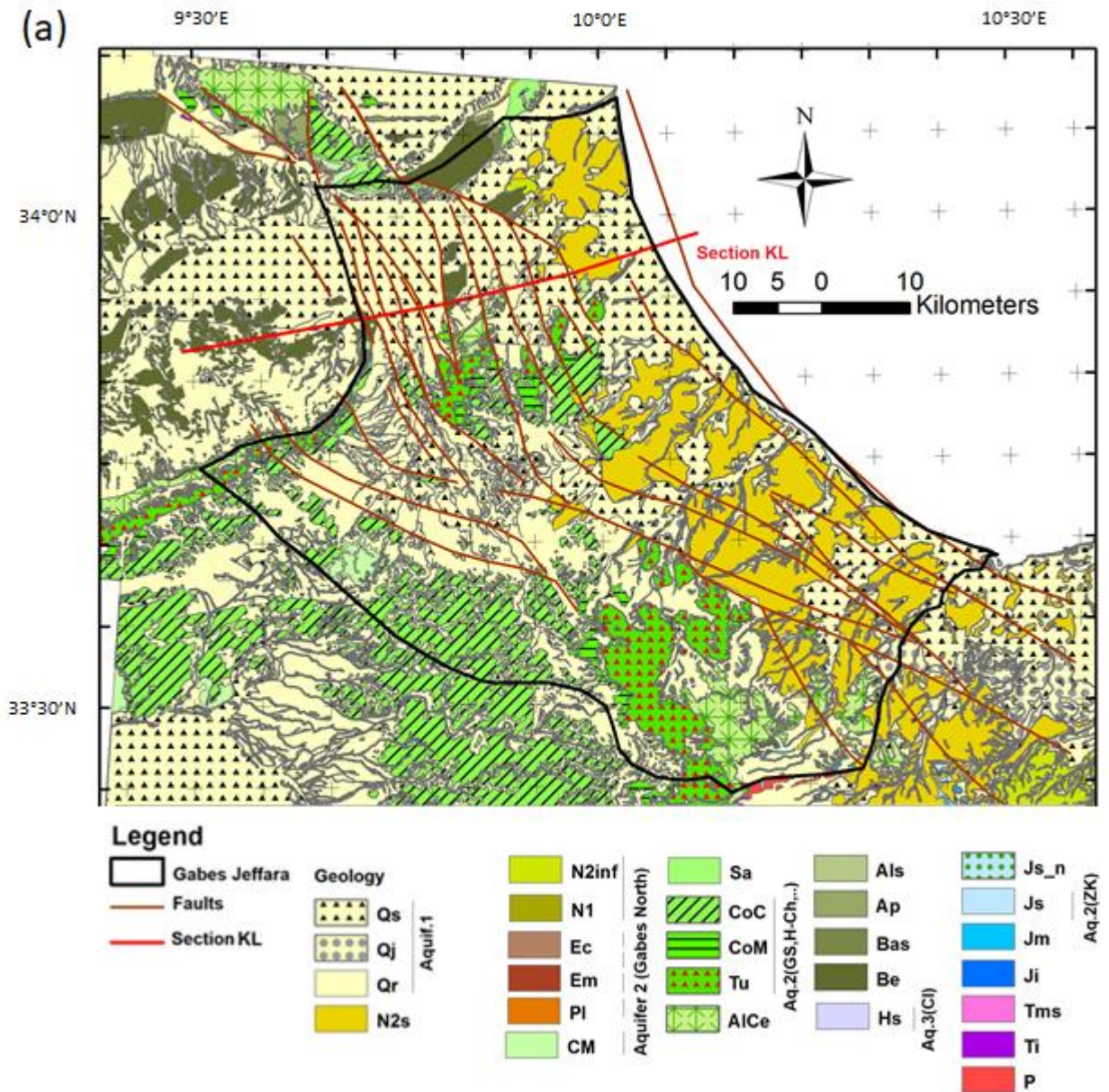


450

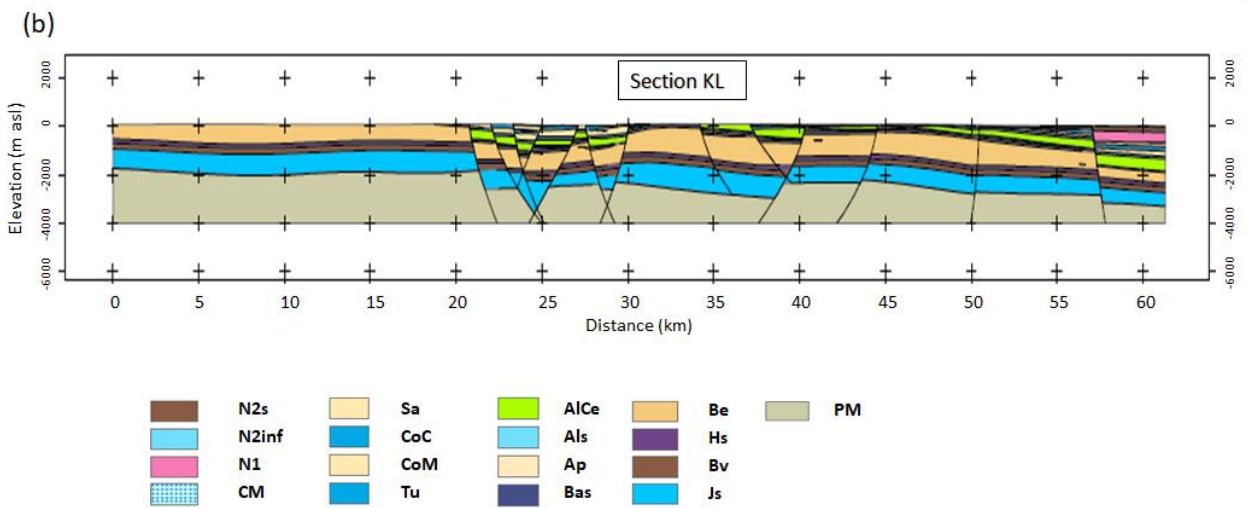
451 **Fig. 1** Location map of the study area, in the governorate of Gabes. Towns: El Hamma (El-Ha); Chenchou (Chen);  
 452 Gabes (Gab); Mareth (Mar); Kettatna (Ket); Toujane (Tou); Matmata (Mat). Wadis (w.): Akarit (Aka); Gabes  
 453 (Gab); Djir (Dji); Zigzaou (Zig); Recifa (Rec); Mjirda (Mji)

454





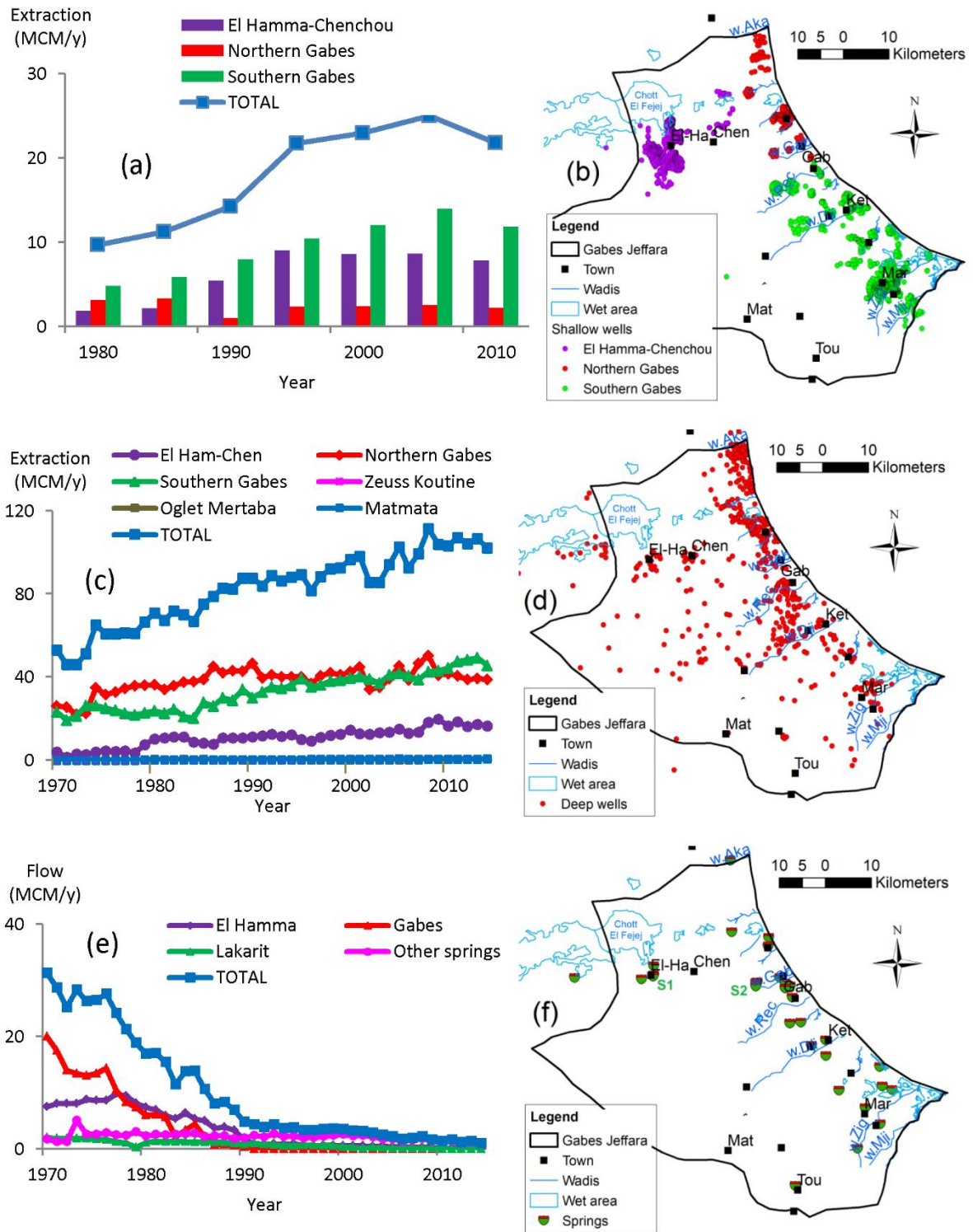
455



456

457 **Fig. 2 (a)** Geological map of the study area and **(b)** cross section passing through Ben Ghilouf, El Hamma, Mettouia  
 458 and Ghannouche. Aquifer 1: Qs : superficial Quaternary, Qj Gabes Jeffara Quaternary, Qr : intra-relief continental  
 459 Quaternary. N2s : lower Pleistocene. Aquifer 2 (Gabes North): N2inf : Pliocene, N1 : Serravallian, CM :

460 Campanian. Sa : Santonian. Aquifer 3 (Gabes South) : CoC : carbonate Coniacian, CoM : marly Coniacian, Tu :  
 461 Turonian. AlCe : Cenomanian – upper Albian. Als : lower Albian. Ap : Aptian. Bas : upper Barremian – lower  
 462 Aptian. Be : lower Barremian. Aquifer 4 : Hs : Hauterivian – Valanginian. Bv : Berriasian-Valanginian. Aquifer 5 :  
 463 Js : upper Jurassic. PM : Permo-Triassic



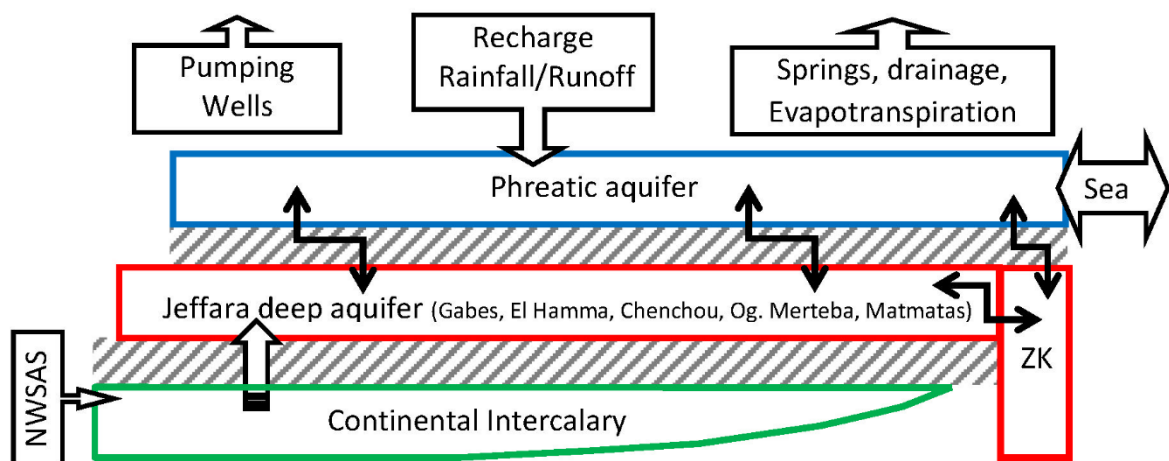
464

465 **Fig. 3** Groundwater exploitation of shallow and deep aquifers: (a) Evolution of shallow aquifer exploitation; (b)  
 466 Location of shallow wells; (c) Evolution of deep aquifer exploitation; (d) Location of deep wells; (e) Evolution of  
 467 spring water flows; (f) Location of springs (S1: El Hamma; S2: Gabes). MCM: million cubic meters. Towns: El

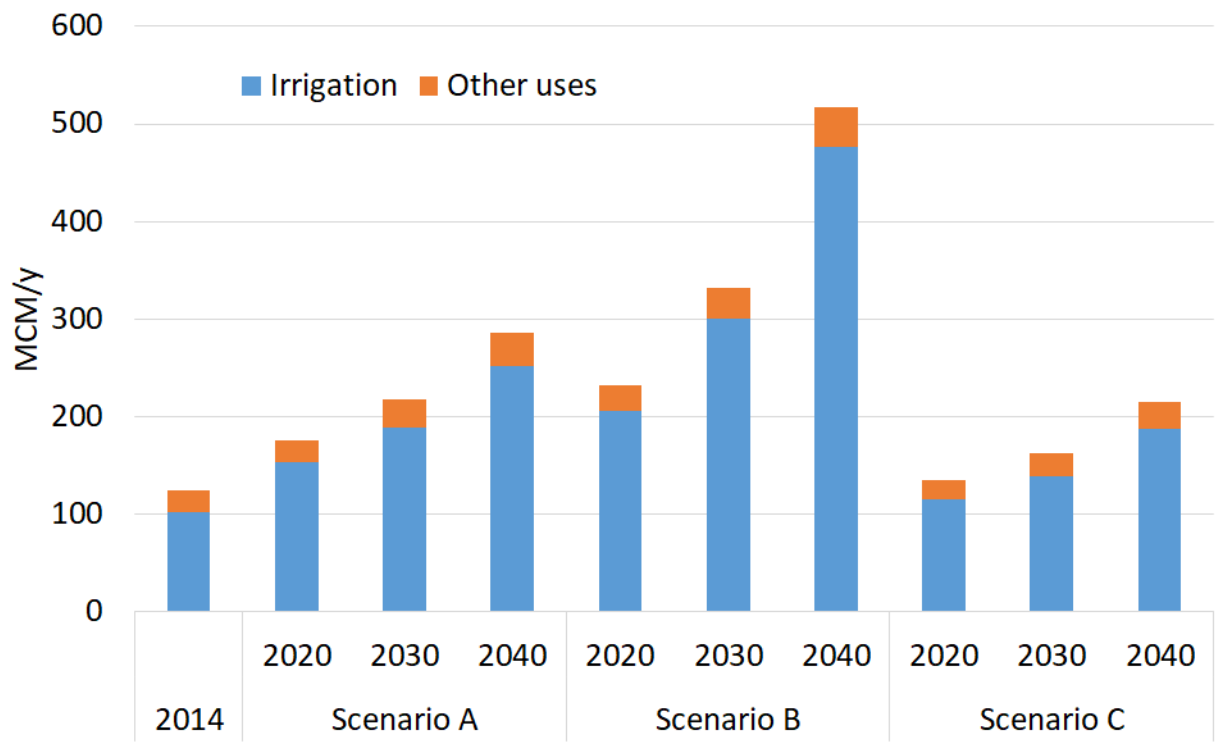
468 Hama (El-Ha); Chenchou (Chen); Gabès (Gab); Mareth (Mar); Kettatna (Ket); Toujane (Tou); Medenine (Med);  
 469 Matmata (Mat). Wadis: Akarit (Aka); Gabès (Gab); Djir (Dji); Zigzaou (Zig); Recifa (Rec); Mjirda (Mji)

Level	Lithology	Geological log	Hydrogeological log	Conceptual model
Quaternary	alluvium	Qs, Qj, Qr	1	aquifer 1 (phreatic)
Lower Pleistocene	marls	N2s	2	
Pliocene	clay sands	N2i	3	
Serravalien	sands	N1	4	aquifer 2 (Jeffara)
Campanian	limestones	CM	5	
Santonian	marls	Sa	6	
Carbonate Coniacian	limestones	CoC	7	
Marly Coniacian	marls	CoM	8	aquifer 3 (Jeffara)
Turonian	limestones	Tu	9	
Cenomanian – upper Albian	marls	AlCe	10	
Lower Albian	sands	Als	11	
Aptian	dolomite	Ap	12	
Upper Barremian – Lower Aptian	sands, sandstone	Bas	13	
Lower Barremian	clays, marls	Be	14	
Hauterivian – Valanginian	sands, sandstone	Hs	15	aquifer 4 (CI)
Berriasian – Valanginian	clays	Bv	16	
Upper Jurassic	limestones	Js	17	aquifer 5 (ZK)
Permo-Triassic	sandstones	PM	18	
Legend of hydrogeological log	medium aquifer	major aquifer	medium aquitard	major aquitard

471 **Fig. 4** Correspondence between the geological model and the hydrogeological model

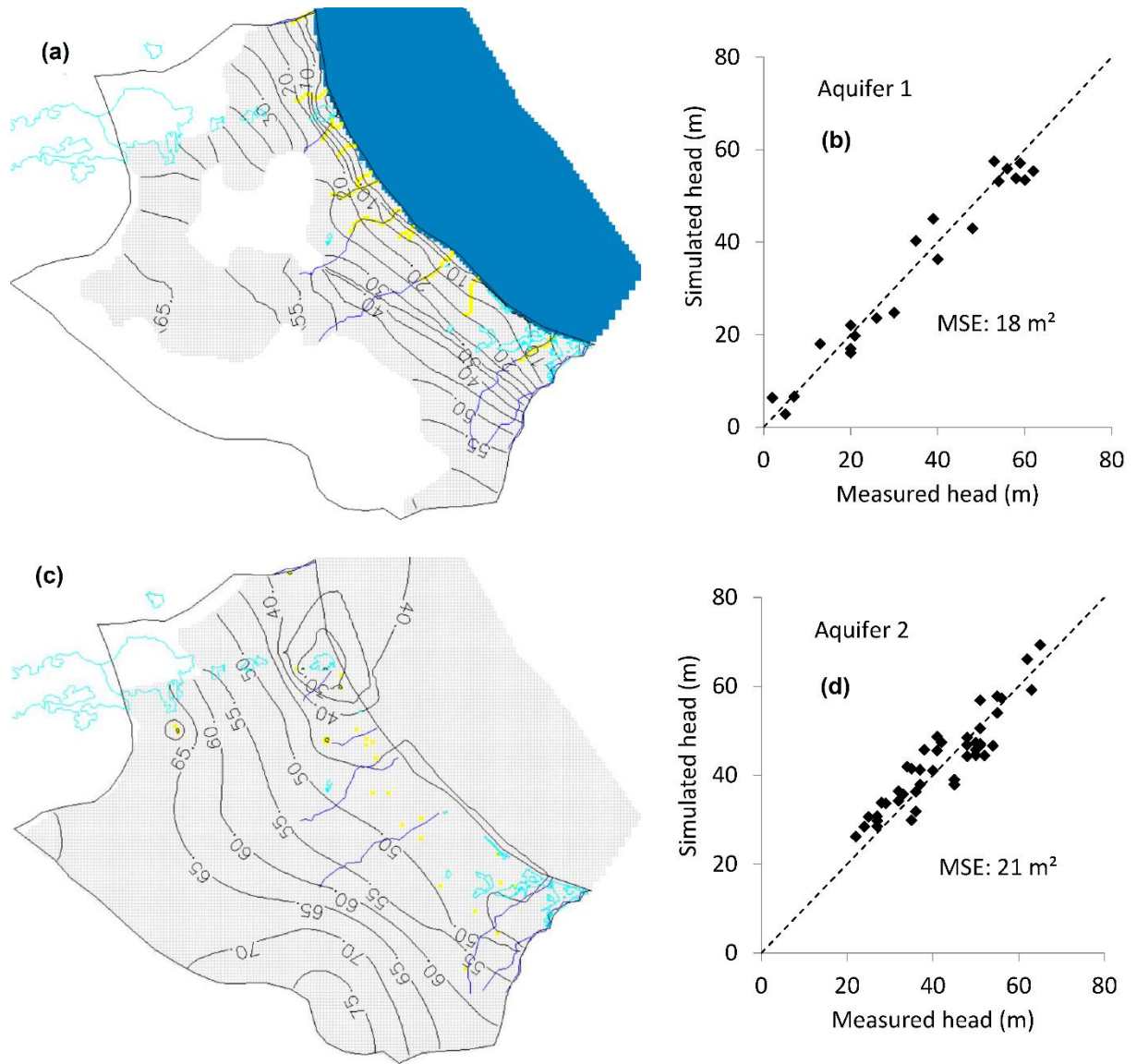


473 **Fig. 5** Conceptual model of Gabes Jeffara aquifer system



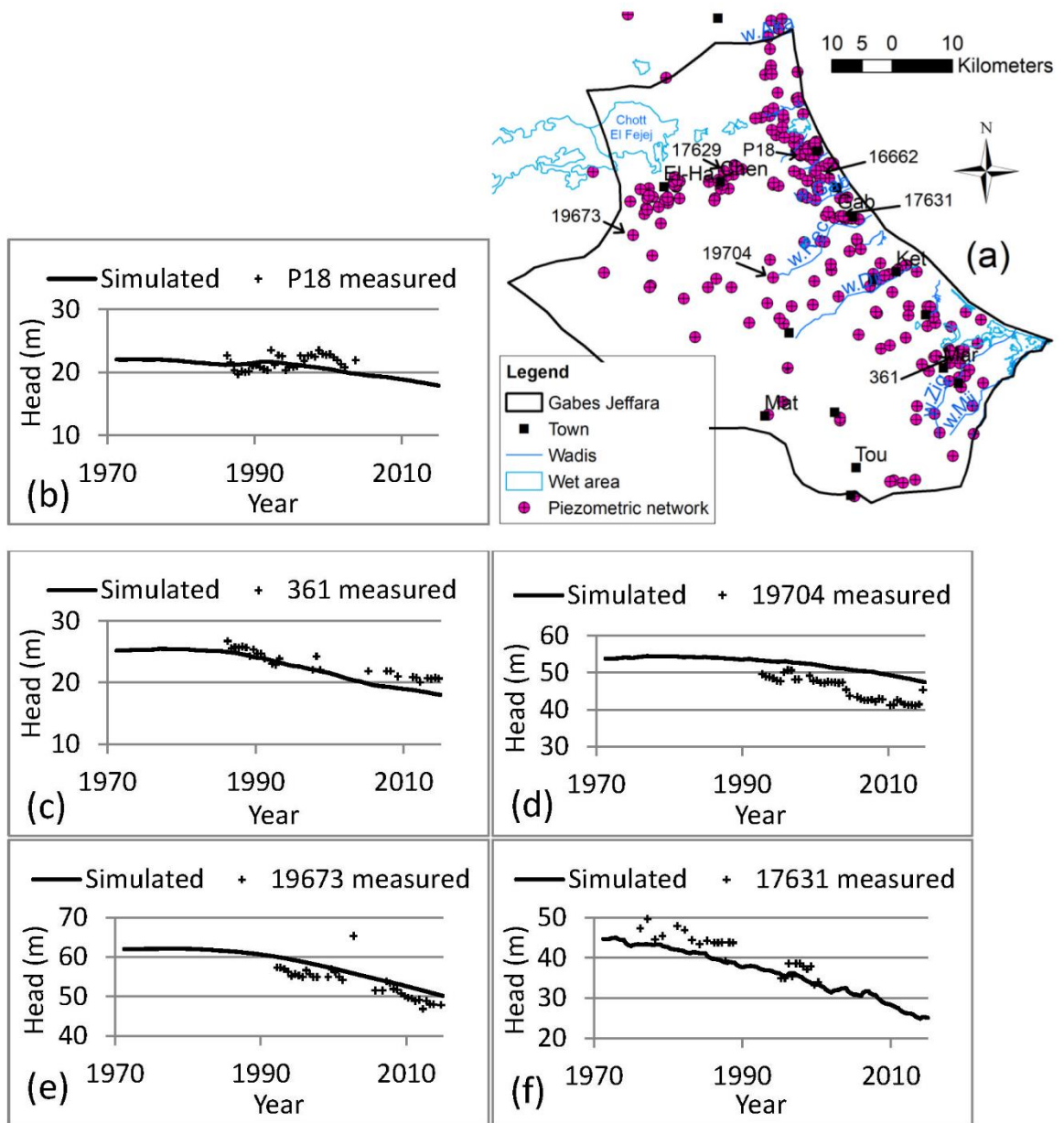
474

475 **Fig. 6** Scenarios of future water demand



476

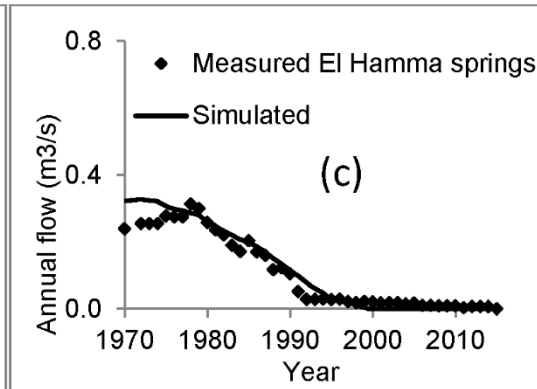
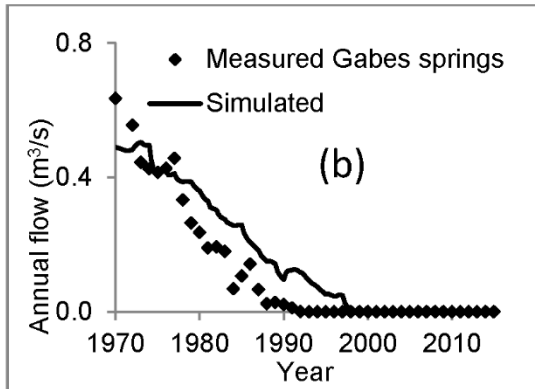
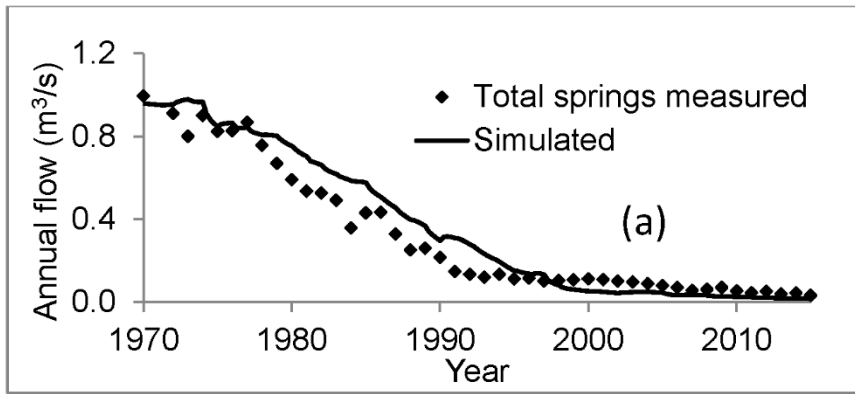
477 **Fig. 7** Steady state calibration: (a) Simulated piezometric map of a shallow aquifer; (b) Simulated vs measured  
 478 heads for a shallow aquifer; (c) Simulated piezometric map of a deep aquifer; (d) Simulated vs measured heads for a  
 479 deep aquifer



480

481 **Fig. 8** (a) Location of groundwater level monitoring wells. Variation of simulated and measured heads at (b) well

482 P18, (c) well 361, (d) well 19704, (e) well 19673, and (f) well 17631

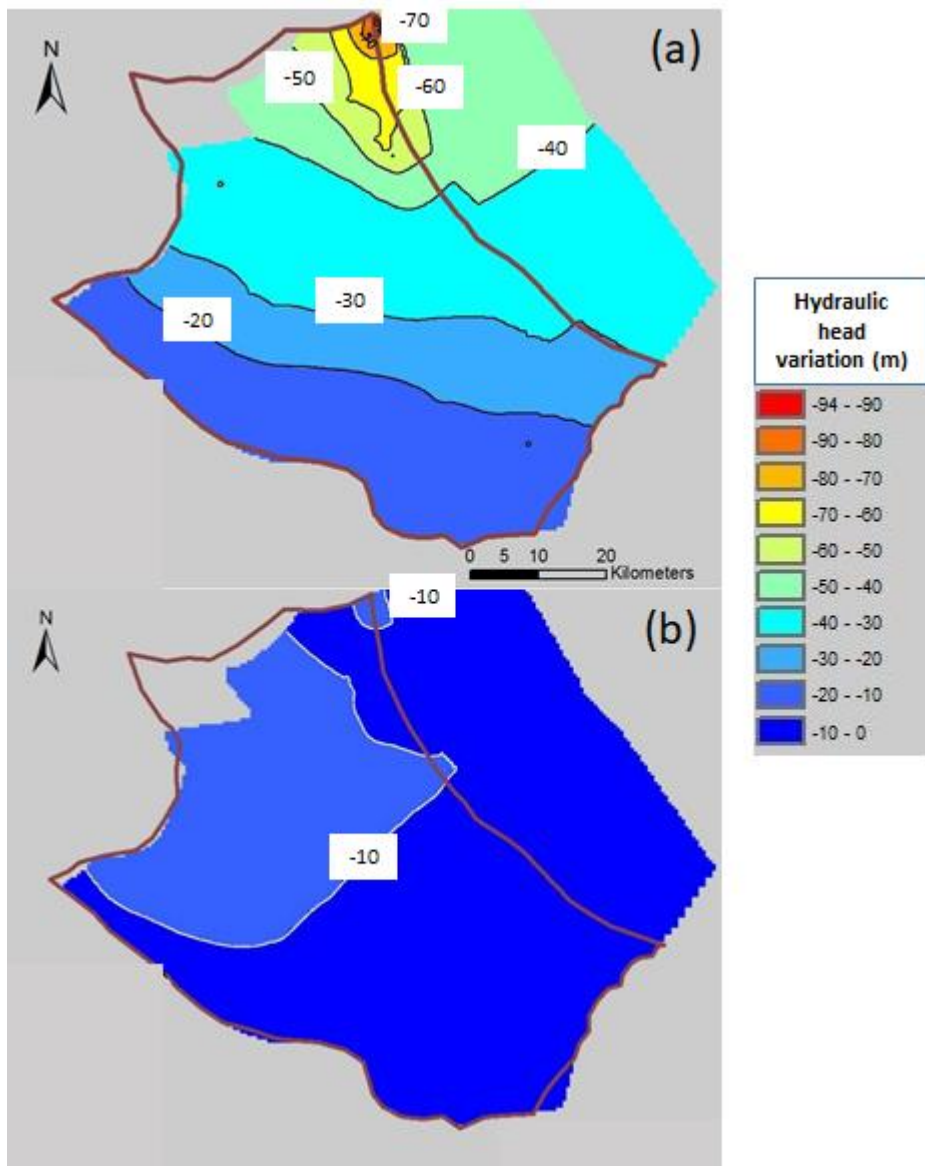


483

484

485

**Fig. 9** Variation of simulated and measured spring flows: (a) total springs, (b) Gabes springs, and (c) El Hamma springs



486

487 **Fig. 10** Variations in simulated hydraulic heads in deep aquifers between 2040 and 2014 for (a) scenario 3 and (b)  
 488 scenario 6

489

490

491